Journal of Soil Sciences and Agricultural Engineering

Journal homepage: www.jssae.mans.edu.eg
Available online at: www.jssae.journals.ekb.eg

Comparison of Thermal Performance Analysis for Single-Slope Solar Stills Using Three Different Depths of Seawater

Abdellatif, S. M.; Y. M. El-Hadidi; G. A. Mosad and Asmaa A. A. Wehba*

Agricultural Engineering Dept., Faculty of Agriculture, Mansoura University

ABSTRACT

In this study an attempt was done to compare the thermal performance for the three identical single-slope solar stills using three different depths of seawater (1, 2, and 3 cm). It was executed under the climatic conditions of Mansoura University (31.045°N latitude angle, and 31.352°E longitude angle, and 6.72 m above the sea level). The experimental work was carried out form the 1st of January until the 19th of April 2020. Different of climatic factors and solar still measurements were monitored, measured and recorded. The hourly average solar energy available inside the solar still wind speed and ambient air temperature during the daylight-time, respectively, was 461.4 W, 1.3 m/s and 21.4ºC. The thermal efficiency for the lowest depth of seawater was higher than that of the other two depths by 22.44% and 49.03%, respectively. The distillation efficiency of the lowest depth of seawater was higher than that of the other depths by 13.34% and 20.15%, respectively. The lowest depth of seawater augmented the productivity rate of freshwater by 42.04% and 77.27% as compared with the other two depths, respectively. The estimated costs of distilled one litre of freshwater from the three different depths of seawater, respectively, were approximately 0.68, 0.96, and 1.20 EGP.

***Keywords*:** Solar energy, seawater, distillation process, passive single-slop solar still.

INTRODUCTION

The rapidly augmenting of population all over the world inducing in big challenges particularly in arid and semiarid districts due to increasing demands of portable water for agricultural operations, industrial activities, and humane utilities. One of the major problems in developing countries is the supplying of portable water. In remote districts of Egypt traditional energy supply is not always possible, where fresh water demands are higher than that in the delta region due to difficulties in reaching fossil fuel to these areas. Moreover, the grid does not occur or the available energy is not enough to operate the distillation units. Uncertain price rise and rapid depletion of fossil fuels accelerated the development of renewable energy sources in the form of alternative power sources (Weldekidan *et al*., 2018).

The rapid population growth approximately 83.0 million persons every year will be increased the energy demands, while the fossil fuel being prevalent the energy sources is estimated to be significantly depleted after 70 years (Metzger and Huttermann, 2009). Today one of the most complex challenges face the humanist is the managing and belting the climatic conditions change produced by over exploitation of natural sources (Morales *et al*., 2014). In Egypt, there are abundant amounts of solar energy have been reached into the earth's surface. Therefore, the use and utilise of new and renewable energy sources given sufficient opportunity of sustainable socioeconomic development by using the resources of a particular district.

Solar energy is one of the most available modes for distilling seawater and its intensity comprehends few forms of heat energy that can be used to drive that process. Portable water needed can easily produces for agricultural and industrial purposes, and drinking as it is cleaner using simple solar still. On an average, each one square meter of the ground surface area can receive enough sunlight which every year can generates power of 1700 kWh. According to Shahsavari and Akbari (2018) the average solar energy flux incident on the horizontal surface in the Middle East district varying approximately between 1800 to 2300 kWh, while in the Europe district, it is only averages about 1200 kWh per square meter per year. Solar energy can provided a significant portion of several industrial and forestry energy demands in several ways such as; electricity and steam generation based upon the photovoltaic technology, and solar thermal technologies (solar water heating systems, solar air heating systems, and solar concentrators) (IEA-ETSAP /IRENA, 2015).

Unfortunately, the amounts of portable water on the earth are fasten firmly and limited (Panchal and Patel, 2017). Approximately, 97% of the total water on the earth is saline water (sea water and the oceans water) while, only about 3% is portable water. Portable water mostly provided in the form of ice (77%), in the two poles (northern and southern poles), 22% is ground water, and only 1% is in rivers and lakes. Agricultural operation consuming approximately 70% of the total fresh water provided for human activities, 20% is using by the industry and only 10% is utilising for household demands (Bataineh, 2016).

The desire freshwater is increased every year, due to high growth of population and upsurge industrialisation. Wastes of industrial and dischargers of sewage mostly discharged in the rivers, therefore, the required freshwater continuously reduced (Panchal and Patel, 2017). Several parameters have been affected the thermal performance and productivity of fresh water from the solar still such as; intensity of solar radiation, temperature potential difference between the glazing material and water, brackish water depth

* **Corresponding author.**
E-mail address: E.Asmaadel@gmail.com
DOI: 10.21608/jssae.2020.135659

in the basin water, insulating material, tilt angle and thickness of the glazing material, and wind speed. Some of the previous factors such as the intensity of solar radiation and wind speed are uncontrolled as they are undergoes to the climatic conditions. The other factors comprehending; the surface area of water basin, depth of saline water in the basin, and insulating material can effectively be controlled and managed for accelerating and enhancing the productivity rate of portable water (Selvaraj and Natarajan, 2018).

The primary objective of this investigation is to study, test, and experimentally examined the possibility of using solar energy for distilling seawater and consequence obtaining and providing the freshwater by using three identical single-slope solar stills with three different depths of seawater.

MATERIALS AND METHODS

This study was executed in the station of Agricultural Researches and Experiments (ARE), Faculty of Agriculture, University of Mansoura at latitude angle of 31.045ºN, longitude angle of 31.352ºE, and mean altitude above the sea level of 6.72 m. The experimental work was carried out from the 1st of January until the 19th of April 2020 to elucidate and determine the best depth can be used for distilling seawater. It was used and utilised many facilities, which providing by the project of "Improvement of Protected Cropping Quantity and Quality Using Renewable Energy Technologies and Bio-Agricultural System" at the same research station.

Experimental Work Materials

Equipment elucidation (single-slope solar still)

The single-slope solar still is considered as the simplest apparatus that is utilised, functioned, and used the solar energy for distilling seawater. Three identical single-slope solar stills were designed and fabricated in a private workshop at Mansoura city, and functioned during this experimentally study for distilling seawater. The three single-slope solar stills were orientated in the direction of East-West to face the south direction and stationary-non tracking. Each single-slope solar still has many technical and active components; bottom and sides, reflector, glazing material, inlet of seawater, and outlet of distilled freshwater, and water jar for collecting the freshwater as shown in Figs (1) and (2). The bottom and sides of single-slope solar still constitute the basin water.

The basin water is made of 2.0 mm thick stainless steel sheet and having a gross dimensions of 90.0 cm long, 40.0 cm wide, and 5.0 cm high with net volume of 18 x 10^3 cm^3. It identifies the absorber plate of solar collectors when acting as an absorber plate of solar radiation. In order to maximise the effective absorptance of the solar radiation flux incident on the bottom of basin water, the upper surface of water basin was coated using matt black paint. Underneath the water basin there is a metallic frame to stand it that is made of 2.5 cm angle iron with 5.0 cm high above the ground. To prevent corrosion of the metallic frame, it was painted by an excellent anti-corrosion paint. To provide and maintain feeding of the seawater into the basin water there is an inlet stainless steel pipe 12.7 mm in diameter that situated on the lateral side of basin. To fetch the condensed freshwater from the inner surface of acrylic cover there is a stainless steel gutter semi-cylindrical in shape, 50.8 mm in diameter witch located just underneath the front inner tilted cover, capped from one side and open from another. Another stainless steel pipe 12.7 mm in diameter was connected to the open side of steel gutter in order to collect the condensed portable water.

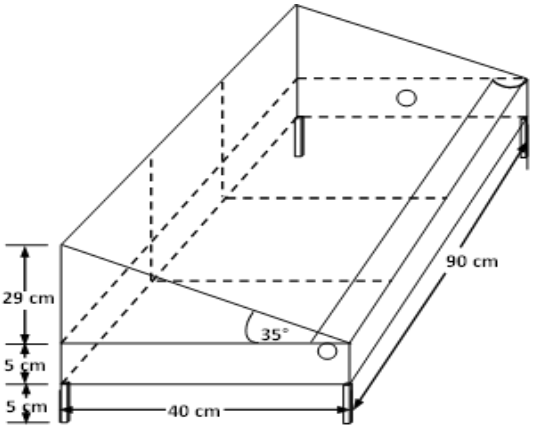

Fig. 1. Schematic diagram of single-slope solar still.

Fig. 2. Three identical passive single-slope solar stills.

The vertical back wall of passive single-slope solar still was covered by nickel chrome sheet that active as a reflector in order to maximise the intensity of solar radiation flux incident on the upper black bottom surface area of basin water and the water itself. Moreover, using the back wall reflector will provide a high thermal trapping in the space heating (space between the top surface of basin water and the inner surface of cover) which accelerating the heating process of seawater during the daylight time. To minimise the heat energy loss or gain of the back vertical wall it was insulated by 2.5 cm thick loosely packed rock-wool insulation which has thermal conductivity of 0.065 W/m ºC.

The front inclined surface and the two triangular vertical sides of solar still was covered using acrylic sheet of 2.0 mm thick which has an effective transmittance and absorptance to short-wave of 0.92 and 0.05, respectively. The front top surface of solar still (acrylic cover) was tilted by 35.0º with the horizontal plane which represents the annual average of optimum tilt angles for the stationary non-tracking solar still. To collect the desalinated fresh water a 5 litres water jar was used. To accelerate and increase the rate of productivity, it was surrounded by a plastic jack spaced 2.5 cm to be filled by a cold water and insulated from the outer surface area by loosely packed rock-wool insulation. To improve and enhance the thermal performance of the passive single-slope solar still, the bottom and sides of basin water were completely insulated using the same insulation material.

Measurements and data Acquisition Unit

To precisely measure and record various variables of atmospheric circumstances such as; ambient air temperature in ºC (ventilated thermistor), solar radiation flux incident on the horizontal plane in W/m^2 (pyranometer), and air speed in m/s (cup anemometer and wind vane), a weather station (Vantage Pro 2, Davis, USA) was utilised. It was situated just beside the solar stills (far away only about 5.0 m). These three different sensors are connected to a data-logger device in order to display and record the desirable data during the experimental work.

These weather data were also update displayed on the video screen by a scan of the three sensors each one minute and recorded the average of five scans on the memory each five minutes by software run to automate transfer the obtained data each one weak throughout the experimental period.

The temperatures of top black plate surface of basin water, seawater, and acrylic cover surface for the three single-slope solar stills were precisely measured using thermocouple type K, displayed, and recorded using a 12-channel data-logger device (Digi-sense scanning thermometer type). These data were also updated and displayed on the video screen by scanning all the sensors each one minute. The average of five scans were also recoded and stored in the memory each five minutes. The obtained data were automate transferred each one weak throughout the experimental work using software run.

For the duration of experimental work, the effect of different atmospheric conditions through various seasons (winter, spring, and summer) was examined. The seawater (water of Mediterranean Sea) was brought down from a location far away asymptotically 100 m from the beach to get pure seawater without any impurities. It was chemically analysed at the central laboratory of Faculty of Agriculture in order to assess the total-soluble-salt (TSS), concentration of hydrogen ion (pH), and any other undesirable elements. The obtained data from the chemical analysis revealed that, the TSS and the concentration hydrogen ion (pH) of the seawater are 32,973 ppm and 8.3, respectively. For the duration of experimental study, three different depths of seawater 1.0 cm (3.6 litres), 2.0 cm (7.20 litres, and 3.0 cm (10.80 litres) were used, tested, and examined to elucidate the influence of seawater depth on the thermal performance and productivity rate of freshwater. These various depths of seawater were also functioned to confirm, specify, and detect the appropriate depth can be used with the passive single-slope solar still under the specific climatic conditions.

Heat Energy Balance on Solar Still

A mathematical model that can be described the heat energy balance on the basin water of passive single-slope solar still is presented as revealed in Fig. (3). It can be assisted and determined the diurnal productivity rate of freshwater and the diurnal overall thermal efficiency of the passive single-slope solar still. The technical specification of the passive single-slope solar still and the factors that used in the computation are summarised and listed in Table (1). The heat energy balance on the seawater in the basin and the basin itself can be described as follows (Velmurugan *et al*., 2009; Kalidasa *et al*., 2010; Duffie and Beckman, 2013; Kabeel *et al*., 2017):

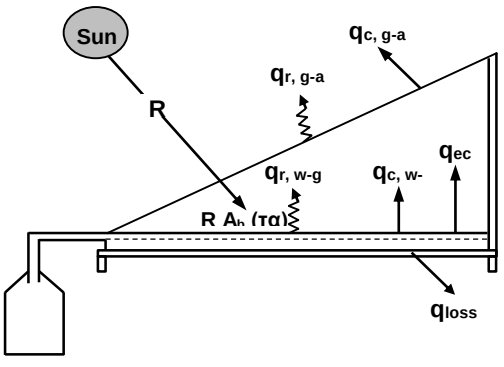

Fig. 3. Schematic diagram of the heat energy balance on the passive single-slope solar still.

$$R\,A_b\,(\tau\alpha) = q_{ec} + q_{c,\,w\text{-}g} + q_{r,\,w\text{-}g} + q_{loss} + m_w\,C_{pw}\,\frac{dT_w}{d\tau} \quad (1)$$

Where, R, is the solar radiation flux incident on tilted surface of solar still in W/m^2, A_b, is the surface area of the basin in m^2, (τα), is the optical efficiency of solar still in decimal, q_{ec}, is the heat energy transfer by evaporation-condensation in W, $q_{c,\,w-g}$, is the convection heat energy transfer between seawater and cover surface in W, $q_{r,\,w-g}$, is the radiation heat energy exchange between seawater and cover surface in W, q_{loss} , is the heat energy loss from the solar still into the ambient air in W, m_w, is the mass of seawater in the basin in kg, C_{pw}, is the specific heat of the seawater in J/kg ºC, and , $dT_w/d\tau$, is the change rate in temperature of seawater at interval time in ºC/s.

Table 1. Some technical specifications of single-slope solar still.

Category	Property	Value
Basin		
	Absorptivity (α), decimal	0.90
	Surface area (A_b), m^2	0.36
	Specific heat (C_{pb}), J/kg ºC	465
	Density (ρ_b), kg/m^3	7830
	Thermal conductivity of insulation (k_i), W/m ºC	0.65
	Thickness of insulation (L_i), m	0.05
	Overall heat transfer coefficient (U_o), W/m^2 ºC	13
	Surface area of sides (A_{sides}), m^2	0.065
Acrylic		
	Thickness of acrylic cover, mm	2.0
	Tilt angle of cover surface, degree	35.0
	Absorptivity of acrylic (α_g), decimal	0.05
	Effective transmittance of acrylic (τ_g), decimal	0.92
	Emissivity of acrylic (ε_g), decimal	0.90
	Surface area of acrylic cover (A_g) , m^2	0.46
Seawater		
	Absorptivity of seawater (α_w), decimal	0.05
	Effective transmittance of water (τ_w), decimal	0.95
	Emissivity of seawater (ε_w), decimal	0.96
	Surface area of seawater (A_w) , m^2	0.36
	Specific heat of seawater (C_{pw}), J/kg ºC	4190
	Density of seawater (ρ_w), kg/m^3	1025

$$q_{ec} = m_D\,A_b\,h_{fg}, \quad W \quad (2)$$

$$m_D = 9.15 \times 10^{-7}\,h_{c,\,w-g}\,(P_{wb} - P_{wg}), \quad kg/m^2\,s \quad (3)$$

$$h_{fg} = 2501.9 - 2.40706\,T_w + 1.192217 \times 10^{-3} T_w^2 - 1.5863 \times 10^{-5} T_w^3, \; kJ/kg \quad (4)$$

Where, m_D, is the mass transfer rate in kg/m^2 s, A_b, is the surface area of basin in m^2, h_{fg}, is the latent heat of evaporation of water in J/kg, $h_{c,\,w-g}$, is the convection heat transfer coefficient between the seawater and the cover surface in W/m^2 ºC, P_{wb}, is the vapour pressure of seawater at water temperature (T_W) in mm Hg, P_{wg}, is the vapour pressure of seawater at cover temperature (T_g) in mm Hg.

$$h_{c,\,w-g} = 0.884\left[(T_w - T_g) + \left(\frac{P_{wb} - P_{wg}}{2016 - P_{wb}}\right) T_w\right]^{1/3}, \; W/m^2\,ºC \quad (5)$$

$$q_{c,\,w-g} = A_b\,h_{c,\,w-g}\,(T_w - T_g), \quad W \quad (6)$$

$$q_{r,\,w-g} = 0.9\,A_b\,\sigma\left(T_w^4 - T_g^4\right), \quad W \quad (7)$$

Where, σ, is the Stefan-Boltzmann constant, 5.67×10^{-8} W/m^2 K^4

$$q_{loss} = U_o\,(A_b + A_{sides})\,(T_p - T_a), \quad W. \quad (8)$$

$$U_o = \frac{k_i}{L_i}, \quad W/m^2\,ºC \quad (9)$$

Where, U_o, is the overall heat transfer coefficient between the basin and ambient air in W/m^2 ºC, A_{sides}, is the surface area of basin sides in m^2, T_p, is the black plate surface temperature in ºC, and, T_a, is the ambient air temperature in ºC.

An energy balance on the cover of solar still, neglecting its heat capacitance and solar energy absorbed by the cover, can be computed as follows:

$$q_{ec} + q_{c,w-g} + q_{r,w-g} = q_{c,g-a} + q_{r,g-s} \quad (10)$$

$$q_{c,g-a} = h_{c,g-a} A_g (T_g - T_a), \quad W \quad (11)$$

$$h_{c,g-a} = 5.7 + 3.8\, v \quad (12)$$

$$q_{r,g-s} = h_{r,g-s} A_g (T_g - T_s), \quad Watt. \quad (13)$$

$$h_{r,g-s} = \varepsilon_g \sigma \left(\frac{(T_g^4 - T_s^4)}{(T_g - T_s)} \right), \quad W/m^2 K. \quad (14)$$

$$T_s = 0.0552 (T_a)^{1.5}, \quad K. \quad (15)$$

Where, $q_{c,g-a}$, is the convection heat transfer between the cover and ambient air, $h_{c,g-a}$, is the convection heat transfer coefficient between cover and ambient air in W/m^2 ºC, A_g, is the surface area of cover in m^2, T_a, is the ambient air temperature, ºC, v, is the wind speed in m/s, $q_{r,g-s}$, is the radiation heat transfer between the cover surface and the sky in W, $h_{r,g-s}$, is the radiation heat transfer coefficient between the cover and sky in W/m^2 K, ε_g, is the emissivity factor of the acrylic cover in decimal, and, T_s, is the sky temperature in K.

The hourly average overall thermal efficiency (η_{th}) of the passive single-slope solar still can be estimated by the following equation:

$$\eta_{th} = \frac{q_{ec}}{R\, A_b\, (\tau\, \alpha)} \times 100, \%. \quad (16)$$

Because of some distillated freshwater may be lost and back again into the basin by dripping from the cover surface or leakage from the collecting trough, therefore, the distillation efficiency can be calculated as follows:

$$\eta = \frac{m\, h_{fg}}{3.6\, R\, A_b\, (\tau\, \alpha)} \times 100, \quad \%. \quad (17)$$

Where, m, is the actual fresh water distillated each hour in kg.

For the duration of the experimental work, the data were measured and stored in the microcomputer files in order to compute all the previous equations and statistically analysed the obtained data using Excel program.

RESULTS AND DISCUSSION

Nowadays, the demands for producing portable water are highly developed due upsurge in the population and industrial growth. Therefore, the desalination technologies are rapidly growing in order to meet these demands of freshwater. There are three different parameters affecting thermal performance and productivity of freshwater from the passive single-slope solar still. These general parameters comprehend; climatic conditions which include solar radiation intensity, ambient air temperature, and wind speed, depth of seawater in the solar still and its temperature. During the desalination process of seawater, there were 1308 hours of bright sunshine of which 984 hours (75.23%) were measured, recorded, and utilised in the distillation process during this experiment.

The hourly averages solar radiation incident on horizontal, inclined surfaces outside the solar stills, inside the solar stills, reflected from the back wall, and the total solar radiation available inside the solar stills during the experimental period are summarised and listed in Table (2). They were 257.4 (±81.0), 377.9 (±133.0), 339.1 (±116.4), 166.7 (±124.0), and 505.8 W (±238.6), respectively. Thus, the nickel chrome back wall increased the available total solar radiation inside the solar stills on an average by 33.70%. While, using the tilt angle of 35º resulting in increasing the solar radiation flux incident on inclined surface by 63.68% as compared with that incident on the horizontal surface. The hourly average intensity of solar radiation varied from hour to hour, day to day, and month to another according to the sky conditions, the solar altitude angle, and the solar incident angle as clarified in Table (2). It was changed from 359.6 W (±183.3) in January to 514.8 W (±264.2) in April.

The hourly average total solar radiation available inside each of the solar still was 359.6 (±183.3), 466.9 (±210.5), 512.6 (±228.7), and 506.6 W (±260), respectively, with an average of 461.4 W (±220.6). These variations occurred due to increasing the solar altitude angles from January (26.7º ±10.0º) to April months (44.4º ±14.4º).

Table 2. Hourly average total solar radiation flux incident on horizontal surface outside (R_{ho}) and inclined surface outside the solar still (R_{io}), inside (R_i), reflected from back wall (R_{ir}), and total (R_{it}) inside the solar still during the experimental period.

Month		Intensity of Solar Radiation, Watt				
		R_{ho}	R_{io}	R_i	R_{ir}	R_{it}
January	Mean	145.8	278.8	252.2	107.4	359.6
	SD	±64.9	±107.4	±102.6	± 81.8	±183.3
February	Mean	196.4	340.8	308.6	158.3	466.9
	SD	±69.0	±108.1	±105.0	±106.8	±210.5
March	Mean	225.7	352.1	318.9	193.7	512.6
	SD	±94.1	±196.7	±104.1	±125.8	±228.7
April	Mean	266.8	394.8	343.9	162.7	506.6
	SD	±81.2	±129.0	±129.3	±138.0	±260.0
Average	Mean	208.7	341.6	305.9	155.5	461.4
	SD	±77.3	±135.3	±110.3	±113.1	±220.6

Because of the intensity of solar radiation is only the main source of heat energy utilised in heating and evaporation of seawater, the temperatures of black basin plate and seawater were increased and decreased as well as the intensity of solar radiation. The hourly average temperatures of black plate, seawater, and cover surface, the latent heat of evaporation of water, thermal efficiency, distillation efficiency, and daily average productivity rate of freshwater for the three different depths of seawater during this experimental work are summarised and listed in Table (3). As the heat energy absorbed by the black plate of water basin augmented it was resulting in increasing the plate temperature according to the intensity of solar radiation available. The black plate temperatures for the three different depths of seawater were increased gradually from 7:00 am until reached the maximum values at 13:00 pm and slowly decreased thereafter. Therefore, the hourly average black plate temperatures for the three different depths of seawater were augmented by 44.1, 40.5, and 34.0ºC at those times, respectively. The hourly average black plate temperatures during this experiment for the three different depths of saline water were 50.7, 47.1, and 43.8ºC, respectively. Consequently, the black plate temperature underneath of 1 cm deep of seawater was increased by 7.64% and 15.75% as compared with the other two depths (2 and 3 cm), respectively. In spite of each solar still was received the same amount of solar radiation, there were differences in the black plate temperatures due to the difference in the capacity of seawater between the three solar stills. As the volume of seawater is decreased the ability of reserving heat energy by the plate increased, then its temperature is augmented.

Table 3. Hourly average temperatures of black plate (T_p), saline water (T_w), acrylic cover (T_g), latent heat of evaporation (h_{fg}), thermal efficiency (η_{th}), distillation efficiency (η) and daily average productivity rate of fresh water (m) for the three different depths during this experimental work.

Month	depth, cm	T_p, °C	T_w, °C	T_g, °C	h_{fg}, kJ/kg	η_{th}, %	η, %	m, ml/m^2/day
Jan.	1	42.8	41.1	29.6	2398.3	44.17	28.53	1070.
	2	39.4	37.9	27.4	2408.7	32.89	24.56	920.0
	3	37.0	35.6.	26.1	2414.5	25.81	17.16	640.0
Feb.	1	51.2	48.7	33.3	2380.5	59.01	47.94	2225.0
	2	46.8	44.9	31.1	2391.0	44.14	30.08	1340.0
	3	44.0	42.3	29.7	2397.7	35.69	24.13	1110.0
March	1	53.3	51.3	34.4	2375.7	64.44	51.48	2780.0
	2	50.9	49.0	33.2	2381.2	55.16	33.54	1805.0
	3	46.1	44.3	30.8	2392.8	43.53	28.52	1530.0
April	1	55.3	53.2	34.2	2376.6	67.01	62.32	2540.0
	2	51.3	49.3	33.4	2380.5	59.43	48.72	2000.0
	3	48.2	46.4	31.8	2387.7	52.41	39.85	1580.0
Average	1	50.7	48.6	32.9	2382.8	58.66	47.57	2153.8
	SD	±13.1	±12.0	±6.7	±26.2	±26.08	±21.20	±204.5
	2	47.1	45.3	31.3	2390.4	47.91	34.23	1516.3
	SD	±12.8	±11.6	±6.5	±30.5	±22.48	±15.98	±177.5
	3	43.8	42.2	29.6	2398.2	39.36	27.42	1215.0
	SD	±11.9	±10.4	±8.4	±27.5	±18.76	±13.27	±138.8

The heat energy absorbed by the black plate underneath the seawater was transferred by natural convection into the water which induced in rising up its temperature. The seawater temperatures for the three different depths of water were augmented gradually from 7:00 am until reached the maximum values at 13:00 pm and slowly decreased after that. The hourly average seawater temperatures during this experiment for the three different capacities of seawater were 48.6 (±12.0), 45.3 (±11.6), and 42.2ºC (±10.4), respectively. So, the lowest depth of seawater was higher than that of the other two depths by 7.28% and 15.17%, respectively. These variations between the three solar stills induced because of the differences in the volumetric heat capacities of seawater (3.6, 7.2, and 10.8 litres). The seawater temperature with the lowest capacity was increased rapidly after sunrise till recognized the maximum value afternoon and rapidly decreased thereafter. Whereas, the other two capacities slowly increased after sunrise until reached the maximum values afternoon and slowly decreased after that.

The temperatures of solar stills cover surface were strongly affected by the seawater temperatures, wind speed, and ambient air temperature surrounding the solar stills. Therefore, the lowest and highest cover temperatures for the three different depths of seawater occurred during January and April months, respectively, as the hourly average ambient air temperatures during January and April months, respectively, were 16.4 (±2.4) and 21.8ºC (±2.9). The hourly average cover temperatures during this experiment for the three different depths of seawater were 32.9 (±6.7), 31.3 (±6.5), and 29.6ºC (±8.4), respectively. The hourly average temperature differences between the cover surface and the ambient air (21.4ºC) for three different depths of seawater during this experiment were 11.5, 9.9, and 8.2ºC, respectively. As a result of these differences, the capability of heat energy transfer by evaporation-condensation for the lowest depth was higher than that of the other two depths.

The thermal performance efficiency of the passive single-slope solar still is the multiply of heat energy transfer by evaporation-condensation and the latent heat of evaporation of saline water divided by the solar energy available inside the solar still (input heat energy). The latent heat of evaporation of water is inversely proportional to the seawater temperature. It varied with respect to time of the day as the seawater temperature was changed. Therefore, the hourly averages latent heat of evaporation of water for the three different depths of water during this experiment, respectively, were 2382.8 (±26.2), 2390.4 (±30.5), and 2398.2 kJ/kg (±27.5). The thermal performance efficiency for the three solar stills with different depths of seawater during this experiment is plotted in Fig. (4). The thermal performance efficiency for three solar stills varied from hour to hour, day to day, and month to another according to the changes in environmental parameters (intensity of solar radiation, wind speed, and ambient air temperature) and experimental factors (depth of seawater and its temperature). It was observed that, the thermal performance efficiency for the three solar stills were increased from 7.00 am till recognized the high level (85.81%) at 14.00 pm for the lowest depth. Whereas, the highest level of thermal performance for the other two depths (77.92% and 66.87%, respectively) were achieved at 15.00 pm due to their heat energy stored in the seawater as evidently elucidated in Fig. (4). The hourly average thermal performance efficiency for the three different depths of seawater, respectively, were 58.66% (±26.08), 47.91% (±22.48), and 39.36% (±18.76). So, the thermal performance efficiency of the lowest depth of saline water was higher than that of the other two depths by 22.44% and 49.03%, respectively, because of the higher volumetric heat capacity.

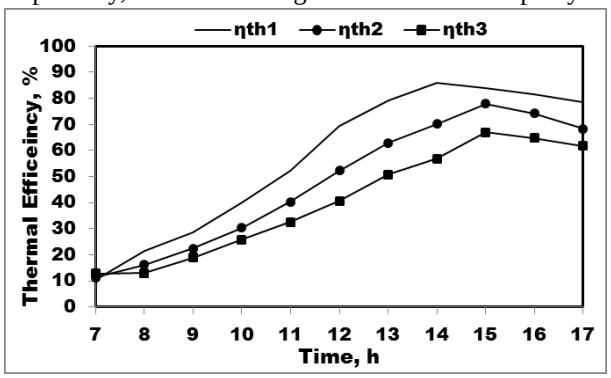

Fig. 4. Hourly average thermal performance efficiencies for the three different depths of seawater during this experiment.

The hourly average freshwater distillated in millilitre during the daylight-time for the three different water depths during this experiment are plotted in Fig. (5). It was augmented gradually from 7.00 am until reached the higher level at 13.00 pm when the seawater temperatures recognized the maximum

values at that time for the three different seawater depths and diminished thereafter. It also observed that the maximum values of fresh water distillated which achieved at 13.00 pm increased from 88.2 to 206.2 ml/h, 69.3 to 159.9 ml/h, and 49.2 to 128.5 ml/h from January to April months for the three different water depths, respectively. These variations occurred because of the increasing in the intensity of solar radiation (from 359.6 W to 506.6 W), and consequently, the increasing in seawater temperatures. The productivity rates of freshwater from the three identical solar stills with three different depths of seawater is strongly affected by the intensity of solar radiation, temperature of seawater, still cover surface temperature, ambient air temperature, and wind speed.

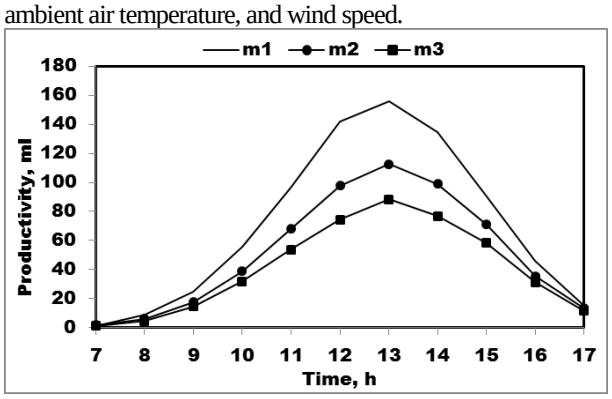

Fig. 5. Hourly average productivity rates for the three different depths of seawater during this experiment.

The productivity rate of freshwater in millilitre per square metre per day during this experiment varied from day to day, and month to another. The diurnal productivity rates of fresh water for the three different seawater depths during this experiment, respectively, were augmented from 1070.0 to 2540.0, 920.0 to 2000.0, and 640.0 to 1580.0 ml/m^2/day from January to April months. These variations in the productivity rates between January and April months were induced because of the seam reason mentioned above. Therefore, the productivity rates of freshwater for the three different depths of water, respectively, were increased from January to April months by 1470.0, 1080.0, and 940.0 ml/m^2/day. The daily average productivity rates for the three different depths of seawater during this experiment were 2153.8 (±204.5), 1516.3 (±177.5), and 1215.0 (±138.8) ml/m^2/day, respectively. As a result to the previous data, the lowest depth of seawater increased the productivity rate by 42.04% and 77.27% as compared with the other two depths, respectively. Accordingly, the productivity rate of fresh water was diminished as the depth of seawater increased. However, it was observed that, the nocturnal productivity rate of the other two higher water depths increased due to the heat energy stored during the daylight hours particularly with higher level of solar radiation as realized in March and April months. As a result of that observation, the nightly average freshwater distillated for the three different seawater depths, respectively, were 500.0, 790.0, and 885.0 ml/m^2/night. These data are agreement with that published by Dsilva *et al.* (2016).

The distillation efficiency of the single-slope solar still is the multiply of the actual freshwater distillated each hour and the latent heat of evaporation of seawater divided by the solar energy available inside the solar still (input heat energy). Due to some of the condensed fresh water for the three similar passive solar stills with three different seawater depths was lost by dripping again into the water basin, the distillation efficiencies were always lower than the thermal efficiency of the solar stills. The hourly average distillation efficiency during the daylight-time for the three different water depths during this experiment is plotted in Fig. (6). The hourly average distillation efficiencies during this experiment varied from hour to hour, day to day and month to another according to the actual fresh water distillated. The daily average distillation efficiency for the three different seawater depths during this experiment, respectively, were augmented from 28.53 to 62.32%, 24.56 to 48.72%, and 17.16 to 39.85% from January to April months. These variations in the distillation efficiency between January and April months were induced due to the previous reasons mentioned previously. Therefore, the distillation efficiency for the solar still with the lowest and highest depths of seawater, respectively, was augmented by 33.79%, 24.16%, and 22.69% from January to April months. It was observed that, the differences between the thermal performance and distillation efficiency diminished with respect to the time from January to April as listed in Table (3). The hourly average distillation efficiency for the three different depths of seawater during this experiment, respectively, was 47.57% (±21.20), 34.23% (±15.98), and 27.42% (13.27). Consequently, the distillation efficiency for the lowest depth was higher than that of the other two depths by 13.34% and 20.15%.

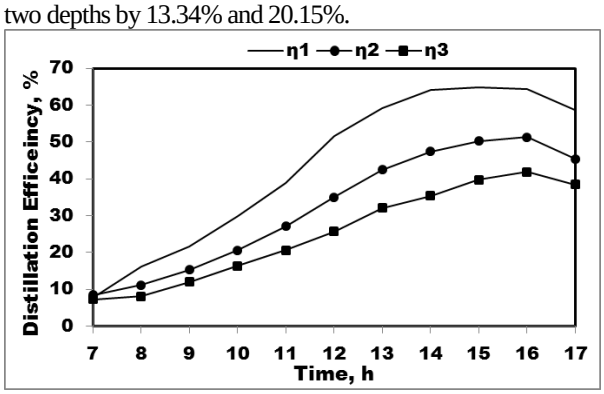

Fig. 6. Hourly average distillation efficiency for the three different depths seawater during this experiment.

The heat energy balance on the seawater in the basin of passive single-slope solar stills was carried out to elucidate the relationship between the input and output heat energy during this experiment. The input heat energy is the solar energy available inside the three passive single-slope solar stills. Whereas, the output heat energy implies the following; heat energy transferred by evaporation-condensation, convection heat energy transfer from the seawater to the cover surface of solar still, radiation heat energy exchange between the seawater and the cover surface, the heat energy loss by convection through both the water basin and sides of basin into the ambient air, and heat energy gained and stored. The input and output heat energy components during this experiment from January to April months are summarised and listed in Table (4). The hourly average total heat energy input (solar energy available inside each of the solar still) during the experimental period, was 461.4 W (±210.0) of which 405.0 (±181.1), 370.1 (±178.1), and 331.6 W (±170.8) was used as an output heat energy for the three different depths of seawater, respectively. Therefore, the hourly averages total output heat energy for the three different depths, respectively, represented 87.78%, 80.21%, and 71.87%. Consequently, 12.22%, 19.79%, and 28.13% of the input heat energy, respectively, was stored in the seawater.

These variations were induced because of the difference in the water capacity (3.6, 7.2, and 10.8 litres) of the three solar stills. As the capacity of saline water is increased the heat energy stored augmented. For the duration of this experiment the relationship between the hourly averages input heat energy are plotted versus the output heat energy as shown in Fig. (7).

Table 4. Hourly average heat energy transferred by evaporation-condensation (q_{ec}), convection heat energy transfer from saline water to cover ($q_{c,w-g}$), radiation heat energy exchange between saline water and cover ($q_{r,\ w-g}$), heat energy loss (q_{loss}), heat energy gained and stored (q_{stored}), and output heat energy (q_{ouput}) for the three different depths of water during this experimental work.

Month	depth, cm	q_{ec}, W	$q_{c,\ w-g}$, W	$q_{r,\ w-g}$, W	q_{loss}, W	q_{stored}, W	q_{output}, W
Jan.	1	105.4	11.0	28.0	174.4	13.0	331.8
	2	85.3	8.6	22.8	146.7	24.9	288.3
	3	78.4	7.4	20.1	131.2	35.4	272.5
Feb.	1	136.9	15.3	36.7	180.9	15.0	384.8
	2	111.1	12.8	31.5	155.5	29.4	340.3
	3	96.6	11.2	28.2	138.4	41.8	316.2
March	1	160.9	17.0	40.2	180.3	14.2	412.6
	2	146.5	15.5	37.2	165.6	26.6	391.4
	3	127.0	12.6	30.7	134.7	33.3	338.3
April	1	216.1	17.1	40.2	197.9	19.6	490.9
	2	186.9	18.7	44.4	88.9	21.1	460.0
	3	156.7	14.8	35.7	177.3	14.7	399.2
Average	1	154.8	15.1	36.2	183.4	15.5	405.0
	SD	±94.5	±7.5	±15.8	±67.3	±45.6	±181.1
	2	132.5	13.9	34.0	164.2	25.5	370.1
	SD	±90.7	±6.8	±14.8	±64.4	±60.2	±178.6
	3	114.7	11.5	28.7	145.4	31.3	331.6
	SD	±75.7	±5.7	±12.7	±55.7	±68.1	±170.8

The heat energy balance on the seawater in the basin of passive single-slope solar still and the basin itself for the three different water depths during this experiment were agreement by 97.25%, 99.45%, and 98.96%, respectively. The plotting data for the three different seawater depths evidently revealed that, the slope of regression equations presented the total heat energy stored in the seawater during the daylight-time. It was presented 8.18%, 9.94%, and 21.69% of the total input heat energy stored in the basin of seawater with coefficients of determination (R^2) of 0.9458, 0.9891, and 0.9794, respectively.

The input thermal capacitance into the acrylic cover of solar still which comprehends the heat energy transferred by evaporation-condensation, convection heat energy transfer from seawater to the cover surface, radiation heat energy exchange between seawater and cover surface. Whereas, the output thermal capacitance from the cover surface into the surroundings includes convection heat energy transfer from the cover surface to the ambient air and radiation heat energy exchange between the cover surface and the sky. The input and output thermal capacitances are summarised and listed in Table (5). The hourly average input thermal capacitance to the acrylic cover (from seawater and basin) and the output thermal capacitance from the cover into the surroundings were changed from hour to hour, day to day, and month to another as listed in Table (5). It clearly indicates that, the input and output thermal capacitances augmented from January to April months as the seawater temperatures and surrounding temperatures (ambient and sky) were increased. The hourly average input thermal capacitance to the cover surface during this experiment for the three different seawater depths, respectively, on an average was 206.1 (±85.1), 180.4 (±76.6), and 154.9 W (±84.9), whereas, the hourly average output thermal capacitance from the outer cover surface into the surroundings for the three different seawater depths on an average was 135.6 (±61.8), 132.7 (±52.9), and 125.3 W (±42.8), respectively. As a result of these differences, the input thermal capacitances into the acrylic cover surface, respectively, were higher than that the rejected thermal capacitance from the cover surface by 51.99%, 35.95%, and 23.62%. Consequently, the input thermal capacitance into the cover surface was always higher than that the output. This is precisely emphasised the point of view that mentioned by Duffie and Beckman (2013), when they revealed that, the capacitance of the covering material is small as compared with that of the seawater and basin.

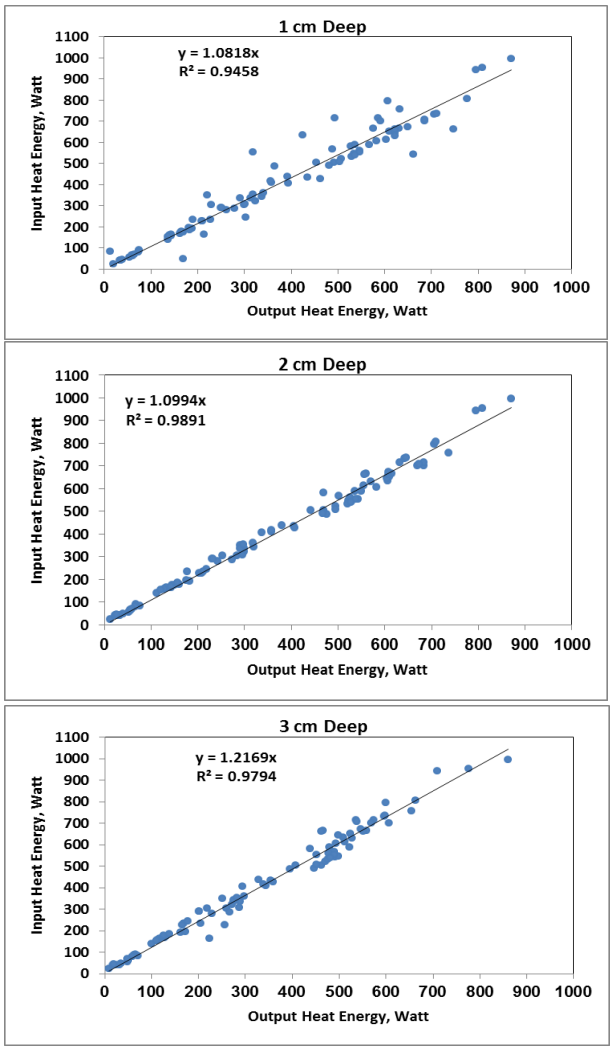

Fig. 7. Hourly average heat energy input as a function of output heat energy for the three different water depths during this experiment.

The relationship between the hourly averages input thermal capacitances to the acrylic cover surface are plotted against the output thermal capacitance from the cover surface into the surroundings (Fig. 8). The heat energy balance on the cover of single-slope solar still for the three different seawater depths during this experiment was correlated together by 85.77%, 90.58%, and 80.06%, respectively. The plotting data for the three different water depths evidently clarified that, the slope of regression equations, respectively, revealed that 52.04%, 35.86%, and 23.55% of the total input thermal

capacitance was stored in the acrylic cover by heat capacitance and solar energy absorbed by the cover during the daylight-time.

Table 5. Hourly average input thermal capacitance into still cover (q_{input}), and output thermal capacitance from the still cover (q_{ouput}) for the three different depths of water during this experimental work.

Month	depth, cm	Input Thermal Capacitance into Cover, W			Output Thermal Capacitance from Cover, W		
		q_{ec}, W	$q_{c, w-g}$, W	$q_{r, w-g}$, W	$q_{c, g-a}$, W	$q_{r, g-s}$, W	q_{output}, W
Jan.	1	105.4	11.0	28.0	47.0	55.2	102.2
	2	85.3	8.6	22.8	42.0	51.6	93.6
	3	78.4	7.4	20.1	42.4	50.8	93.2
Feb.	1	136.9	15.3	36.7	58.2	70.2	128.4
	2	111.1	12.8	31.5	53.9	63.0	116.9
	3	96.6	11.2	28.2	52.5	62.3	114.8
March	1	160.9	17.0	40.2	68.6	74.7	143.3
	2	146.5	15.5	37.2	70.8	76.8	147.6
	3	127.0	12.6	30.7	67.7	70.1	137.8
April	1	216.1	17.1	40.2	80.5	88.0	168.5
	2	186.9	18.7	44.4	81.7	90.9	172.6
	3	156.7	14.8	35.7	72.4	82.8	155.2
Average	1	154.8	15.1	36.2	63.6	72.0	135.6
	SD	±94.5	±7.5	±15.8	±32.5	±12.1	±61.8
	2	132.5	13.9	34.0	62.1	70.6	132.7
	SD	±90.7	±6.8	±14.8	±34.4	±11.1	±52.9
	3	114.7	11.5	28.7	58.8	66.5	125.3
	SD	±75.7	±5.7	±12.7	±29.7	±8.9	±42.8

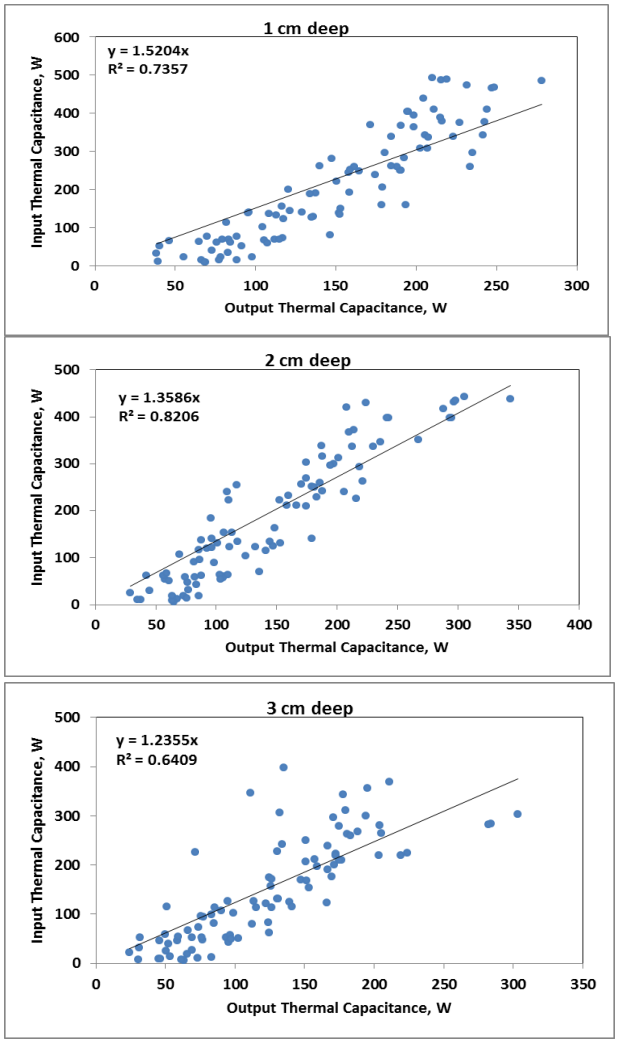

Fig. 8. Hourly average input thermal capacitance as a function of the output thermal capacitance for the three different water depths during this experiment.

For the duration of this study, the seawater (Mediterranean Sea), the total-soluble-salt in the water was substantially diminished from 32,973 ppm to on an average 52.9 ppm in the distillation freshwater. However, the concentration hydrogen ion (pH) was slightly reduced from 8.3 to on an average 7.5 in the fresh water during the experimental work. The total-soluble-salt in the portable water for drinking or irrigating different crops is gave a good determination for the quality of water. As a result the quality of freshwater identifies to the level that recommended by WHO (2004).

Cost Assessment

The fixed costs of one passive single-slop solar still components imply; iron frame, stainless steel sheet, nickel chrome sheet, acrylic cover sheet, insulation material, stainless steel pipes for feeding the seawater into the basin and collecting the fresh water, and finally the labour costs of fabricating solar still. The total fixed costs were about EGP 1,850. Whereas, the salvage value per square metre per year of the fixed costs was about 487.5 EGP with depreciation rate of 10.54%. During this experiment the daily averages productivity rate for the three different depths of seawater (1, 2, and 3cm), respectively, were 2.154, 1.516, and 1.215 litres per square metre. The solar still may be operated 335 days per year according to the sunshine hours and the circumstances of environmental parameters during the experimental work. The annual total productivity rates for the three different depths are 721.59, 507.86, and 407.03 litre sper square metre, respectively. Therefore, the computed costs of one litre distilled of freshwater from the passive single-slope solar still for the three different depths of seawater, respectively, were approximately 0.68, 0.96, and 1.20 EGP/litre.

CONCLUSION

Based on the obtained results from the present study, the following conclusions can be pointed out as:

(1) Using the tilt angle of 35º for the solar still cover resulting in augmenting the solar radiation flux incident by 46.81% as compared with that incident on the horizontal surface. While, using the reflector of nickel chrome increased the available total solar radiation on an average by 32.96%.

(2) The black plate temperature underneath of 1 cm deep of seawater was higher than that of the other two depths by 7.64% and 15.75%, respectively. While, the seawater temperature with 1 cm deep was higher than that of the other two depths by 7.28% and 15.17%, respectively.

(3) The temperature potential differences between the cover surface and the ambient air, respectively, were 11.5, 9.9, and 8.2ºC. As a result of these differences, the ability of heat energy transfer by evaporation-condensation for the lowest depth was higher than that of the other depths.

(4) The hourly average thermal performance efficiencies for the three different depths of seawater, respectively, were 58.66%, 47.91%, and 39.36%. So, the thermal performance efficiency for the lowest depth of seawater was higher than that of the other two depths by 22.44% and 49.03%, respectively, due to the higher volumetric heat capacity.

(5) The hourly averages distillation efficiency for the three different depths of seawater during this experiment, respectively, were 47.57%, 34.23%, and 27.42%.

(6) The daily average productivity rates for the three different depths of water were 2.154, 1.516, and 1.215 l/m^2/day,

respectively. So, the lowest depth of seawater increased the productivity rate by 42.04% and 77.27% as compared with the other two depths, respectively. The lowest productivity rate in the large depths occurred because it was taken long time during the daylight-time to warm up the large volume of seawater.

(7) The total-soluble-salt in the seawater was substantially diminished from 32,973 ppm to on an average 52.9 ppm in the distillation freshwater.

(8) The estimated costs of distilled one litre of freshwater for the three different depths of water, respectively, were approximately 0.68, 0.96, and 1.20 EGP.

REFERENCES

Bataineh, K. M. (2016) "Multi-effect desalination plant combined with thermal compressor driven by steam generated by solar energy" Desalination, 385: 39 – 52.

Duffie, J.; and Beckman, W. (2013) "Solar Engineering of Thermal Processes" 4th edition, John Wiley and Sons, New York, USA

IEA-ETSAP/IRENA (2015) "Solar heat for industrial processes" Technology brief E21

Kabeel, A. E.; Omara, Z. M.; and Essa, F. A. (2017) "Theoretical with experimental validation of modified solar still using Non-fluids and external condenser" journal of the Taiwan Institute of Chemical Engineers, 1: 1 – 10.

Kalidasa, M., K.; Sivakuumar, S; RiazAhmed, J. Chockalingam KnKSK; and Srithar, K. (2010) "Single basin double slope solar still with different minimum basin depth and energy storing materials" Applied Energy, 87: 514 – 523

Metzger, J. O.; and Huttermann, A. (2009) "Sustainable global energy supply based on lignocellulosic biomass from afforestation of degraded areas" Naturwissenschaften, 96: 279 – 88.

Morales, S.; Miranda, R.; Bustos D.; Cazares T.; and Tran H., (2014) "Solar biomass pyrolysis for the production of bio-fuels and chemical commodities" J Anal Appl Pyrolysis, 109: 65 – 78.

Panchal, H. N. ; and Patel, S. (2017) "An extensive review on different design and climatic parameters to increase distillate output of solar still" Renewable and Sustainable Energy Reviews, 69: 750 – 758.

Selvaraj, K.; and Natarajan, A. (2018) "Factors influencing the performance and productivity of solar stills- A review" Desalination, 435: 181 – 187.

Shahsavari, A.; and Akbari, M. (2018) "Potential of solar energy in developing countries for reducing energy-related emissions" Renewable and Sustainable Energy Reviews, 90: 275 – 291.

Velmurugan,V.; Mandlin J.; Stalin, B.; and Srithar, K. (2009) "Augmentation of saline streams in solar stills integrating with a mini solar pond" Desalination, 249(1): 143 – 149.

Weldekidan, H.; Strezov, V.; and Town, G. (2018) "Review of solar energy for biofuel extraction" Renewable and Sustainable Energy Reviews, 88: 184 – 192

World Health Organisation (WHO), (2004) "Guidelines for drinking-water quality" 3rd edition: Volume 1- Recommendation. Geneva. ISBN: 978- 92-4-154761-1.

مقارنة تحليل الإداء الحرارى للمقطرات الشمسية المائلة من جهة واحدة بإستخدام سمك مختلف للماء المالح

صلاح مصطفى عبد اللطيف ، ياسر مختار الحديدى ، غادة على مسعد و أسماء عادل وهبة*

قسم الهندسة الزراعية – كلية الزراعة – جامعة المنصورة

تتناول هذه الدراسة إستغلال الطاقة الشمسية فى تقطير مياه البحار بإستخدام المقطرات الشمسية الخاملة والمائلة من جهة واحدة بزاوية ميل مقدارها 35º . تم تصميم وتصنيع ثلاث وحدات متشابهة من المقطرات الشمسية أبعاد حوض الماء لكل وحدة 90 x40 cm وتم تغطية السطح المائل والجوانب بطبقة من الإكليرك المسطح بسمك 2 mm تم إجراء التجارب بمحطة التجارب والبحوث الزراعية بجامعة المنصورة عند خط عرض 31.05ºN وخط طول 31.37ºE فى الفترة من أول يناير وحتى 19 إبريل 2020م. تقييم الأداء الحرارى للمقطرات الشمسية الخاملة شمل تحديد الكفاءة الحراية وكفاءة عملية التقطيروالإنتاجية اليومية من الماء المقطر وآخيراً إتزان الطاقة على الماء المالح وحوض المقطر وأيضاً غطاء المقطر وذلك لثلاثة مستويات مختلفة من سمك الماء (1, 2, and 3 cm) أوضحت النتائج المتحصل عليها من التجارب العملية لهذه الدراسة ما يلى: 1-إستخدام زاوية الميل 35º لغطاء المقطر الشمسى أدى إلى زيادة كمية الأشعة الشمسية الساقطة على الغطاء بنسبة 46.81% مقارنة بتلك المقاسة على سطح أفقى، بينما أدى إستخدام عاكس النيكل كروم إلى زيادة كمية الطاقة الشمسية المتاحة بنسبة 32.96% 2-درجة حرارة اللوح الأسود أسفل ماء البحر بسمك 1 cm كان أعلى من السمكين الآخرين بنسبة 15.75% and 7.64% على التوالى، كما كانت درجة حرارة الماء المالح لسمك 1 cm أعلى من السمكين الآخرين على التوالى بنسبة 15.17% and 7.28% 3-الفارق الكلى فى درجة الحرارة بين غطاء المقطرات الشمسية والهواء الخارجى المحيط بها كانت على التوالى 11.5, 9.9, and 8.2ºC وكنتيجة لهذا الفارق فإن قابلية إنتقال الحرارة بالتبخير والتكثيف لأقل سمك كانت أعلى من السمكين الآخرين. 4-بلغ متوسط الساعة لكفاءة الأداء الحرارى لثلاثة مقطرات خلال هذه التجربة .58.66%, 47.91%, and 39.36% على التوالى، لذا لإغن كفاءة الأداء الحرارى للمقطر مع سمك ماء مقداره 1 cm كانت أعلى من كفاءة الأداء الحرارى لسمكين الآخرين بنسبة 22.44% and 49.03% على التوالى.5- نتيجة لأن بعض الماء المكثف على الغطاء الداخلى للمقطرات الشمسية يتم فقده من خلال التساقط مرة آخرى فى حوض المقطر لذا فإن كفاءة التقطير تكون أقل قيمة من كفاءة الأداء الحرارى. لذلك فإن متوسط الساعة لكفاءة التقطير للثلاثة مقطرات كانت 47.57%, 34.23%, and 27.42% على التوالى.6- بلغ المتوسط اليومى لإنتاجية المقطرات الشمسية الثلاثة 2.154, 1.516, and 1.215 l/m^2/day على التوالى، لذا فإن معدل الإنتاجية من الماء المقطر للسمك الأصغرمن الماء المالح كان أعلى من السمكين الآخرين بنسبة 42.04% and 77.27% على التوالى.7- تركيز الملح الذائب الكلى فى ماء البحر قبل التقطير كان 32,973 ppm وإنخفض بعد التقطير إلى 52.9 ppm للثلاث معاملات المختلفة للمقطرات الشمسية.8- حساب التكاليف للتر الواحد من الماء المقطر للمعاملات الثلاثة المختلفة كانت 0.68, 0.96, and 1.20 EGP. على التوالى.